

Dynamics and active control of chemical oscillations modeled as a forced generalized Rayleigh oscillator with asymmetric potential

J. A. Adéchinan^{1*}, Y. J. F. Kpomahou², C. H. Miwadinou³ and L. A. Hinvi⁴

¹Département de Physique, Faculté des Sciences et Techniques de Natitingou, UNSTIM-Abomey, Bénin.

²Department of Industrial and Technical Sciences, LARPET, ENSET-Lokossa, UNSTIM- Abomey, Bénin

³Department of Physics, ENS-Natitingou, UNSTIM- Abomey, Bénin

⁴Département de Génie Mécanique et Productique, Institut National Supérieur de Technologie Industrielle (INSTI) Lokossa, UNSTIM-Abomey, Bénin

*Corresponding author E-mail: adjos85@gmail.com

Abstract

This paper focuses on the dynamics and active control of chemical oscillations governed by a forced generalized Rayleigh oscillator. The Melnikov method is used to analytically determine the critical parameters for the onset of chaotic motions. The analytical results are confirmed by numerical simulations. The bifurcation structures obtained show that the model displays a rich variety of dynamical behaviors and remarkable routes to chaos. The effects of the control gain parameters on the behavior of the system are analyzed and the results obtained have shown the control efficiency.

Keywords: Chemical oscillations, Generalized Rayleigh oscillator, Melnikov chaos, Coexisting attractors, Active control.

1. Introduction

Chaos theory is one of the most exciting and rapidly expanding research topics of recent decades [1]. Chaos occurs only in deterministic nonlinear dynamical systems. Indeed, from a theoretical perspective, virtually anything that happens over time could be chaotic [2–6]. In the literature, studies of chaos [3, 5, 7–10] and the nonlinear dynamic phenomena have been carried out in several areas (physics, mathematics, communications, chemistry, biology, physiology, medicine, ecology, hydraulics, geology, engineering, atmospheric sciences, oceanography, astronomy, the solar system, sociology, literature, economics, history, international relations, and in other fields). This sufficiently shows the multidisciplinary character of chaos theory. Obviously, the control of chaos in nonlinear oscillations appears today an important subject of investigation for scientific community because of its multiple applications in various fields.

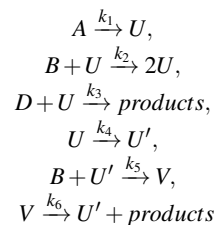
In chemistry, most of the studies carried out on oscillating chemical reactions have revealed non-equilibrium phenomena such as complex oscillations, bistability, and quasi-chaotic behavior [11]. The different types of motion obtained in nonlinear systems are mostly dependent on several factors including: the nature of the nonlinearity, the choice of system parameters and the initial conditions [12–15]. It is therefore important to suppress or if possible control the sources of instabilities in some systems in order to be able to use them in applications. To this end, depending on the nature of the problem considered, several control techniques have been developed in the literature [16–19]. These methods are: OGY-method, passive controls, active controls and semi-active controls. The work carried out on the active control technique is the most numerous [20]. However, research is also actively continuing on other control techniques. Recent studies have used the passive method to control chaotic behavior. For example, Olabodé et al. [21] used the passive control technique to suppress the instabilities occurring during regular and chaotic oscillatory states of plasma. These authors have shown that the oscillatory states being sources of instability of the plasma, a passive control technique would be appropriate to regulate both the chaotic oscillations and the high amplitude of the oscillations which can occur respectively in chaotic and non-chaotic states. Olabodé et al. [22] studied the passive control of horseshoes chaos in dissipative nonlinear chemical oscillations. Using the BZ reactions, they showed how the stress parameter of the nonlinear chemical system, the control parameter and the fluid seep can affect the critical conditions for the appearance of chaotic movements obtained when the passive control force is applied.

We consider in this work the Briggs-Rauscher reaction model. It belongs to a category of nonlinear chemical reactions well developed in the scientific literature. We made this choice because it has already been demonstrated that a modified Van der Pol-Duffing oscillator can be used to model the nonlinear chemical oscillations like BZ reactions [21–26]. Since the control of regular and irregular motions is an interesting issue in several areas [27], the dynamical behavior of a forced generalized Rayleigh oscillator, which constitutes a new model for describing the nonlinear chemical oscillations, may be investigated. For this, we use the Melnikov method to analyze the chaotic behavior of this new chemical oscillator. By acting on certain control parameters, we hope to significantly reduce or eliminate the chaotic behavior in order to bring the chemical system to a stationary state or a state of regular motion. The focus of this work is therefore to improve the understanding and strengthen the knowledge on the horseshoes chaos and active control in nonlinear chemical oscillations modeled by a forced generalized Rayleigh oscillator with asymmetric potential. The originality of this work is brought by the introduction of impure (x^2) and pure (x^3) cubic damping terms to modified Van der pol-Duffing oscillator recently used in the chaotic dynamics of nonlinear chemical oscillations. The structure of this research paper is arranged as follows: in Section 2, we present the model, equilibrium points and their stabilities. In Section 3, we derive the Melnikov criterion for homoclinic chaos. Bifurcation structures and routes to chaos are investigated in Section 4. In Section 5, we apply an active control strategy to suppress or reduce the chaotic behavior in our chemical system. The last section is devoted to the conclusion of this work.

2. Model, equilibrium points and their stabilities

2.1. Model

The generic model for nonlinear oscillations used in this study is based on the kinetic scheme which given by the following chain of equations [21, 22, 28, 29]:



where, the incoming fluxes of the respective species A, B , and D , and the inverse of the resident time, k_1 , are controlled externally. It has been shown that, if one derives the kinetic equations under the assumptions of the law of mass action, steps (1)-(4) may give a bistability and that steps (4)-(6) may be handled as a feedback on the constraint parameter of the autocatalytic step, inducing oscillations of the studied type for suitable values of the amplitude feedback parameter, k_5 [28]. We will assume thereafter that the sink of the product is a first order reaction. Thus, using the laws of mass action and conservation, we get after some mathematical transformations that the self-oscillations in some nonlinear chemical systems can be defined as follows:

$$\begin{cases} \dot{u} = -u^3 + \mu_0 u - kv - \lambda, \\ \dot{v} = \frac{u - v}{\tau} \end{cases} \quad (1)$$

where u and v designate the concentration of the two intermediate species, λ is the constraint parameter because it acts as constant negative feedback for the system, k is the second constraint parameter on which feedback values depend and τ is the characteristic evolution time of the feedback $-kv$. Several nonlinear phenomena (bifurcations, multistability, chaotic behavior, etc.) appear when reactive chemical species act with the catalytic surface. To study these complex phenomena, many works [30] suggest to model by nonlinear oscillator equations such as for example the Van der Pol oscillator which is widely used. By adopting the same approach, we aim to reduce the number of species needed to control the dynamics of chemical reactions described by Eq. (1). Taking into account Eq. (1) and using the following similar linear transformation equations made in [4]

$$\begin{cases} x = v, \\ y = \frac{1}{\tau} [-\mu_0 u + (k - \mu_0)v] \end{cases} \quad (2)$$

with

$$\dot{x} = y, \quad (3)$$

we obtain after some algebraic manipulations, a generalized Rayleigh oscillator equation:

$$\ddot{x} - \mu \left(v - x^2 + \eta x \dot{x} - \frac{1}{3} \eta^2 \dot{x}^2 \right) \dot{x} + \alpha x + \beta x^3 - \gamma = 0 \quad (4)$$

where $\gamma = \frac{\lambda \mu_0}{\tau}$, $\beta = \frac{(\mu_0 - k)^3}{\tau \mu_0}$, $\eta = \frac{\tau}{\mu_0 - k}$, $v = \frac{\mu_0(1 + \tau \mu_0) - k}{3\tau(\mu_0 - k)^2}$, $\mu = 3 \left(1 - \frac{k}{\mu_0} \right)^2$ and $\alpha = \frac{1}{\mu_0 \tau^2} [(\mu_0 - k)(2\mu_0 - k) - \tau \mu_0^3]$ Since several studies have shown that when the system is subjected to an external excitation, many dynamic behaviors appear, we have taking into account in this paper an external sinusoidal excitation of the form $F \cos(\omega t)$. Thus the new chemical oscillator can be written through Eq.(4) as follows:

$$\ddot{x} - \mu \left(v - x^2 + \eta x \dot{x} - \frac{1}{3} \eta^2 \dot{x}^2 \right) \dot{x} + \alpha x + \beta x^3 - \gamma = F \cos(\omega t) \quad (5)$$

where x , \dot{x} and \ddot{x} represent respectively the displacement, velocity and acceleration. F and ω are respectively the amplitude and the frequency of the parametric and external excitations. For the specific case where $\gamma = \eta = 0$, $\mu = -\mu$ and if $\nu = 1$, Eq.(5) is reduced to the equation of classical Van der Pol-Duffing oscillator. In addition, it is important to underline that Eq.(5) contains a specific case used in [31]. At present, we investigate in the following subsection the equilibrium points and their stabilities.

2.2. Equilibrium points and their stabilities

We determine in this subsection the equilibrium points of the autonomous chemical system given by Eq.(4) as well as their stabilities. To determine the equilibrium state, it is necessary to set the condition $\dot{x} = \dot{y} = 0$ [32]. So, we found as equilibrium state $S = (x_e, 0)$ where x_e the fixed point verifies the following equation:

$$x_e^3 + px_e + q = 0 \quad (6)$$

where $p = \frac{\alpha}{\beta}$ and $q = -\frac{\gamma}{\beta}$. The roots of Eq.(6) can be derived as:

$$x_{e1} = \xi_1 \sqrt[3]{-\frac{q}{2} + \sqrt{\Delta}} + \xi_2 \sqrt[3]{-\frac{q}{2} - \sqrt{\Delta}} \quad (7)$$

$$x_{e2} = \sqrt[3]{-\frac{q}{2} + \sqrt{\Delta}} + \sqrt[3]{-\frac{q}{2} - \sqrt{\Delta}} \quad (8)$$

$$x_{e1} = \xi_2 \sqrt[3]{-\frac{q}{2} + \sqrt{\Delta}} + \xi_1 \sqrt[3]{-\frac{q}{2} - \sqrt{\Delta}} \quad (9)$$

where $\Delta = \frac{q^2}{4} + \frac{p^3}{27}$, $\xi_1 = \frac{-1 + j\sqrt{3}}{2}$, $\xi_2 = \frac{-1 - j\sqrt{3}}{2}$. According to cadran discriminant, when $\Delta > 0$, there exists one equilibrium point, which can be obtained from Eq.(8). However, the autonomous chemical system given by Eq.(4) possesses two equilibrium points when $\Delta = 0$. For $\Delta < 0$ Eq.(6) admits three equilibrium points, which can be obtained from (7)-(8).

In order to determine the stability of each equilibrium point, it is necessary to linearize Eq.(4) around equilibrium points. Thus, the Jacobian matrix around equilibrium points is given by:

$$J = \begin{bmatrix} 0 & 1 \\ -\alpha - 3\beta x_e^2 & \mu(\nu - x_e^2) \end{bmatrix} \quad (10)$$

Thus, the characteristic equation associated to the previous matrix is:

$$r^2 + Y(x_e)r + Z(x_e) = 0 \quad (11)$$

where $Y(x_e) = \mu(x_e^2 - \nu)$ and $Z(x_e) = \alpha + 3\beta x_e^2$. If D is the discriminant of Eq.(11), then we have: $D = Y^2(x_e) - 4Z(x_e)$. Therefore, the eigenvalues r solution of Eq.(11) are given by

$$r_{1,2} = -\frac{1}{2}Y(x_e) \pm \frac{1}{2}\sqrt{D} \quad (12)$$

From Eq.(12), the stability of the equilibrium points can be analyzed not only according to the sign of D but also of the sign Y of and Z . Then we have the following possibilities:

- when $D > 0$ and $Z < 0$ Eq.(11) has two real roots with opposite signs, which implies that the equilibrium point is an unstable saddle point;
- when $D < 0$, $Y > 0$ and $Z > 0$, Eq.(11) has two real roots with negative signs. Thus, the equilibrium point is a stable saddle point;
- when $D < 0$ and $Y > 0$, then Eq.(11) has a pair of complex conjugate roots with negative real parts, which indicates that the equilibrium point is a stable node-focus;
- when $D < 0$ and $Y < 0$, Eq.(11) has a pair of complex conjugate roots with positive real parts, which means that the equilibrium point is an unstable node-focus;
- when $Y = 0$ and $Z > 0$, Eq.(11) has a pair of pure imaginary roots which implies the presence of two Hopf bifurcation points with $x_e = \pm\sqrt{\nu}$ with $\nu > 0$.
- when $Y > 0$ and $Z = 0$, it appears in the chemical system governed by Eq.(4), two fold bifurcation points $x_e = \pm\sqrt{\frac{-\alpha}{3\beta}}$ for $\alpha < 0$ and $\beta > 0$.

To verify numerically these above results, we consider the case where the autonomous chemical system given by Eq.(4) admits three equilibrium points. In this consideration, we use the following parameter values: $\alpha = -1$, $\beta = 0.85$, $\gamma = 0.3$, $\nu = 0.1$ and $\mu = 0.01$. Thus, the equilibrium points and their stabilities are given in Table. 1

Table 1: Stability of the equilibrium points S_1, S_2 and S_3 obtained in the case where Eq.(4) admits three different equilibrium points.

Equilibrium points	Eigenvalues	Stability
$S_1 (-0.8808, 0)$	$r_{1,2} = -0.0034 \pm 0.0067j$	Stable
$S_2 (1.2115, 0)$	$r_{1,2} = -0.0068 \pm 0.0227j$	Stable
$S_3 (-0.3308, 0)$	$r_1 = 3.2820e - 0005,$ $r_2 = -1.2682e - 0004$	Unstable

3. Horseshoe chaos

3.1. Melnikov criterion for homoclinic chaos

According to several authors, when a nonlinear oscillator is subjected to an external excitation, there appears the transition from regular to irregular motion [33]. It is noteworthy that the important criterion to observe this passage can be obtained from Melnikov’s theory [34] which is a powerful analytical tool used in several studies to detect chaotic dynamics and analyze near-homoclinic motion with deterministic or random perturbation. The unperturbed system of equation (4) can be written as follows:

$$\begin{cases} \dot{x} = y, \\ \dot{y} = -\alpha x - \beta x^3 + \gamma \end{cases} \tag{13}$$

The asymmetric potential function associated to our system is given by:

$$V(x) = \frac{1}{2}\alpha x^2 + \frac{1}{4}\beta x^4 - \gamma x. \tag{14}$$

The unperturbed system is Hamiltonian, and associated Hamiltonian is:

$$H(x, y) = \frac{1}{2}y^2 + V(x) \tag{15}$$

The homoclinic orbits which connect the fixed points of unperturbed system correspond to zero Hamiltonian. Thus, by solving the equation $H(x, y) = 0$, these orbits are given by the following components [35]:

$$\begin{cases} x_h = p + \frac{\sqrt{2}\sigma^2}{\beta [p \pm q \cosh(\sigma\tau)]}, \\ y_h = \mp \frac{\sqrt{2}q\sigma^3 \sinh(\sigma\tau)}{\beta [p \pm q \cosh(\sigma\tau)]^2} \end{cases} \tag{16}$$

where $p = \frac{\gamma}{2\alpha} \sqrt{\frac{-3\beta}{\alpha}}$, $q = \sqrt{\frac{-1}{2\beta} (2\alpha + \beta p^2)}$, $\sigma = \sqrt{\frac{-1}{2} (2\alpha + 3\beta p^2)}$, $\tau = t - t_0$ and t_0 is the cross-section time of the Poincaré map and can be considered as the initial time of the forcing time. We have plotted in Fig.1, the potential (Fig. 1(a)) as well as the homoclinic orbits (Fig. 1(b)) of the system of Eq.(13). From Fig. 1(a), we notice that the depth of right well increases when γ increases.

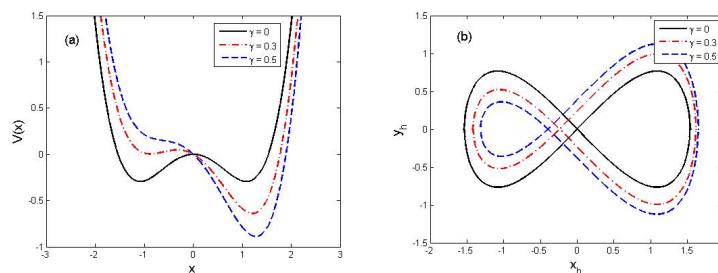


Figure 1: (a)-Potential function $V(x)$ and (b)-homoclinic orbits for three different values of γ with $\alpha = -1$ and $\beta = 0.85$.

Second, we have assumed that the unperturbed system discussed above is perturbed by nonlinear damping and external excitation forces. We therefore apply the Melnikov criterion to predict analytically the horseshoes chaos in our chemical system. We put equation (5) in the form:

$$\begin{cases} \dot{x} = y, \\ \dot{y} = -\alpha x - \beta x^3 + \gamma + \mu \left(v - x^2 + \eta xy - \frac{1}{3}\eta^2 y^2 \right) y + F \cos(\omega t) \end{cases} \tag{17}$$

According to several authors, the Melnikov function is defined by:

$$M(t_0) = \int_{-\infty}^{\infty} f(x_h, y_h) \wedge g(x_h, y_h) dt, \tag{18}$$

where the vectors g and f are given respectively by:

$g \left(\mu \left(v - x^2 + \eta xy - \frac{1}{3} \eta^2 y^2 \right) y + F \cos(\omega t) \right)$ and $f \left(\alpha x + \beta x^3 - \gamma \right)$ The Melnikov integral can therefore be written as follows:

$$M(t_0) = \mu \left[v \int_{-\infty}^{\infty} y_h^2 d\tau - \int_{-\infty}^{\infty} x_h^2 y_h^2 d\tau - \eta \int_{-\infty}^{\infty} x_h y_h^3 d\tau - \frac{1}{3} \eta^2 \int_{-\infty}^{\infty} y_h^4 d\tau \right] d\tau + F \int_{-\infty}^{\infty} y_h \cos(\omega t) d\tau. \quad (19)$$

By setting: $I_1 = \int_{-\infty}^{\infty} y_h^2 d\tau$, $I_2 = \int_{-\infty}^{\infty} x_h^2 y_h^2 d\tau$, $I_3 = \int_{-\infty}^{\infty} x_h y_h^3 d\tau$, $I_4 = \int_{-\infty}^{\infty} y_h^4 d\tau$, $I_5 = \int_{-\infty}^{\infty} y_h \cos(\omega t) d\tau$, the Melnikov function becomes:

$$M(t_0) = \mu \left[v I_1 - I_2 - \eta I_3 - \frac{1}{3} \eta^2 I_4 \right] + F I_5. \quad (20)$$

For the determination of the integrals I_1, I_2, I_3 and I_4 we set $x = \sigma \tau$, $\pm \frac{q}{p} = \frac{\sqrt{\lambda^2 - 1}}{\lambda}$ and we used the following formulas which are obtained from the standard integral tables [36]:

$$\int_0^{\infty} \frac{\sinh^{2\mu} x}{\left(l + \sqrt{l^2 - 1} \cosh x \right)^{\nu+1}} dx = \frac{2^\mu e^{-i\mu\pi} \Gamma(\nu - 2\mu + 1) \Gamma(\mu + \frac{1}{2})}{\sqrt{\pi} (l^2 - 1)^{\mu/2} \Gamma(\nu + 1)} Q_{\nu-\mu}^\mu(l), \quad \nu - 2\mu + 1 > 0, R_e(\mu + 1) > 0, \quad (21)$$

where $Q_{\nu-\mu}^\mu(l) = \frac{e^{j\mu\pi} \sqrt{\pi} \Gamma(\nu + 1)}{2^{\nu+1} \Gamma(\nu + \frac{3}{2})} (l^2 - 1)^{-(\nu-\mu+1)/2} F \left(\frac{\nu+1}{2}; \frac{\nu-2\mu+1}{2}; \nu - \mu + \frac{3}{2}; \frac{1}{1-l^2} \right)$. In this expression, $\Gamma(Z)$ is the Gamma function, $Q_{\nu-\mu}^\mu(l)$ is the associated Legendre function of the second kind and $F(a; b; c; l)$ is the hyper-geometric function. So, we obtain for these first four integrals the following expressions:

$$I_1 = \frac{4\sigma^5}{15\beta^2 q^2} F \left(2; 1; \frac{7}{2}; \frac{q^2 - p^2}{q^2} \right)$$

$$I_2 = \frac{4\sigma^5 p^2}{15\beta^2 q^2} F \left(2; 1; \frac{7}{2}; \frac{q^2 - p^2}{q^2} \right) + \frac{16\sigma^9}{315\beta^4 q^4} F \left(3; 2; \frac{11}{2}; \frac{q^2 - p^2}{q^2} \right) + \frac{16\sqrt{2} p \sigma^7}{105\beta^3 q^3} F \left(\frac{5}{2}; \frac{3}{2}; \frac{9}{2}; \frac{q^2 - p^2}{q^2} \right)$$

$$I_3 = 0$$

$$I_4 = \frac{16\sigma^{11}}{1155\beta^4 q^4} F \left(4; 2; \frac{13}{2}; \frac{q^2 - p^2}{q^2} \right)$$

Then, we determine the last integral I_5 of the Melnikov function using another formula given by:

$$\int_0^{\infty} \frac{\cos(\omega \tau)}{p \pm q \cosh(\sigma \tau)} d\tau = \frac{\pi \sin \left(\frac{\omega}{\sigma} \cosh^{-1} \left(\frac{P}{q} \right) \right)}{\sigma \sqrt{p^2 - q^2} \sinh \left(\frac{\omega \pi}{\sigma} \right)}. \quad (22)$$

After a few mathematical operations we obtain:

$$I_5 = \frac{2\sqrt{2}\sigma\omega\pi \sin(\omega t_0)}{\beta \sqrt{p^2 - q^2} \sinh \left(\frac{\omega \pi}{\sigma} \right)} \sin \left(\frac{\omega}{\sigma} \cosh^{-1} \left(\frac{P}{q} \right) \right).$$

Inserting the expression of integrals I_1, I_2, I_3, I_4 and I_5 into Eq.(20) the Melnikov function can be written as follows:

$$M(t_0) = A \pm BF \sin(\omega t_0), \quad (23)$$

where

$$A = \frac{4\mu\sigma^5}{15\beta^2 q^2} (1 - p^2) F \left(2; 1; \frac{7}{2}; \frac{q^2 - p^2}{q^2} \right) - \frac{16\mu\sigma^9}{315\beta^4 q^4} F \left(3; 2; \frac{11}{2}; \frac{q^2 - p^2}{q^2} \right) - \frac{16\sqrt{2}\mu p \sigma^7}{105\beta^3 q^3} F \left(\frac{5}{2}; \frac{3}{2}; \frac{9}{2}; \frac{q^2 - p^2}{q^2} \right) - \frac{16\sigma^{11}}{1155\beta^4 q^4} F \left(4; 2; \frac{13}{2}; \frac{q^2 - p^2}{q^2} \right)$$

$$B = \frac{2\sqrt{2}\sigma\omega\pi}{\beta \sqrt{p^2 - q^2} \sinh \left(\frac{\omega \pi}{\sigma} \right)} \sin \left(\frac{\omega}{\sigma} \cosh^{-1} \left(\frac{P}{q} \right) \right).$$

If $M(t_0) = 0$ for some t_0 , then horseshoes exist, and chaos occurs. Using this Melnikov criterion it is found that chaos appears when the following condition is satisfied:

$$F \geq F_{cr} = \left| \frac{A}{B} \right| \quad (24)$$

Fig.2 shows the variation of the amplitude of the external excitation versus the frequency. It is noteworthy that the area located below the curve (F_{cr}, ω) indicates the domain where the forced generalized Rayleigh oscillator has a regular behaviour, and above this curve, the oscillator has a chaotic behavior. In short, for the fixe value of the frequency, the critical value F_{cr} for the appearance of Smale's horseshoe chaos increases with μ and ν (see Figs.2(b) and 2(c)). In other words, the area where the horseshoes chaos appears decreases when the parameters μ and ν increases. However, as γ increases, this area increases (see Fig. 2(a)).

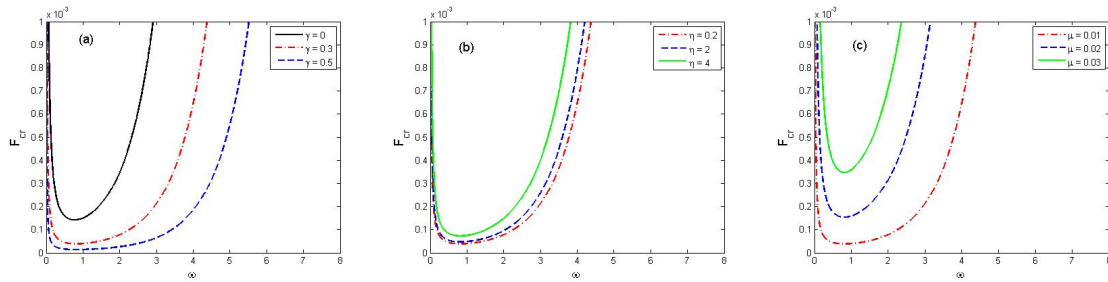


Figure 2: Critical amplitude versus the frequency for appearance of the Melnikov chaos showing the effects of : (a)- γ ; (b)- η and (c)- μ . The basic values are: $\alpha = -1$, $\beta = 0.85$, $\gamma = 0.8$, $\nu = 0.1$, and $\mu = 0.01$.

3.2. Fractal Basin Boundaries

To test the validity of analytical predictions, several authors suggest numerically studying the regular and irregular shape of the basins of attraction. Thus, we solve numerically Eq.(5) by using the fourth order Runge-Kutta algorithm and the results obtained are presented in Figs3-6. Fig.3 shows the influence of the amplitude of the external excitation on the basin of attraction of the generalized Rayleigh oscillator with asymmetric double well potential. We note that the basin of attraction exhibits a regular form when the amplitude of the external excitation is chosen in regular domain predicted by Fig.2. However, the basin of attraction is destroyed and the fractal behavior becomes more and more visible when the value of the amplitude of the external periodic excitation is chosen in chaotic region.

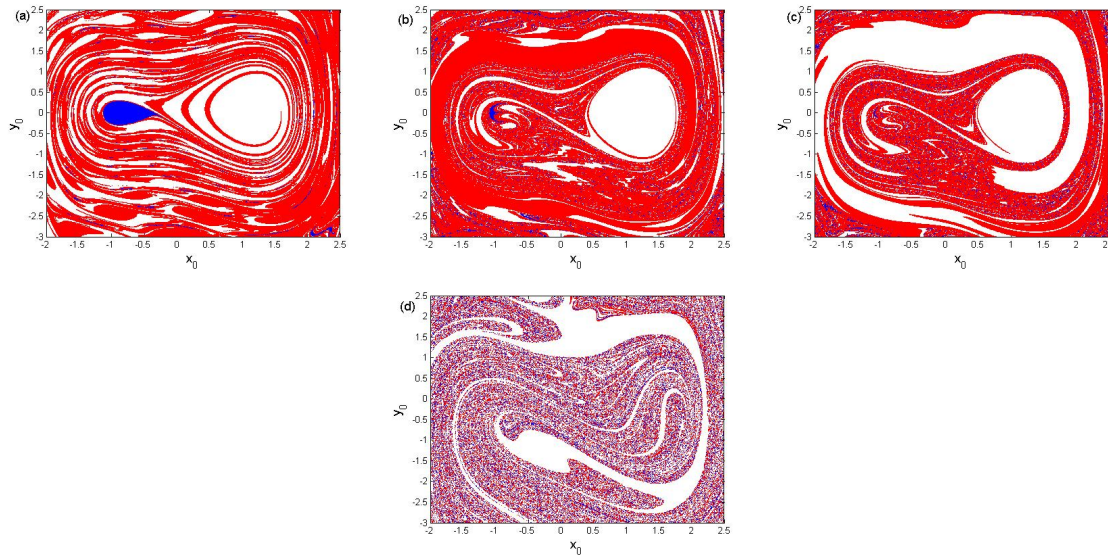


Figure 3: Basins of attraction of a forced generalized Rayleigh oscillator under asymmetric double well potential with the parameters of Fig.4 for (a) $F = 0.00003$, (b) $F = 0.07$, (c) $F = 0.09$ and (d) $F = 0.85$

We can therefore conclude that the analytical and numerical predictions are in good agreement. We wish to investigate how the basins of attraction of the chemical system under consideration are affected as the parameters γ , η and μ vary. From Fig.4 we clearly see that the chaotic behavior accentuates when γ increases. However when the nonlinear damping coefficients η and μ increase the erosion of the basin of attraction decreases implying the decreasing of the chaotic behavior (see Figs.5 and 6).

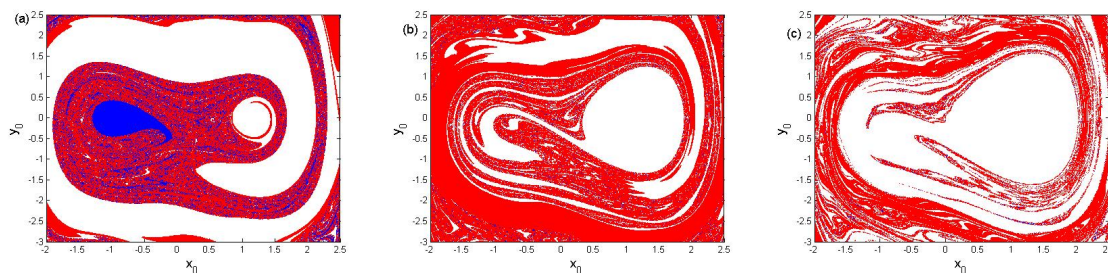


Figure 4: Effect of γ on the basin of attraction: (a) $\gamma = 0$, (b) $\gamma = 0.4$ and (c) $\gamma = 0.6$.

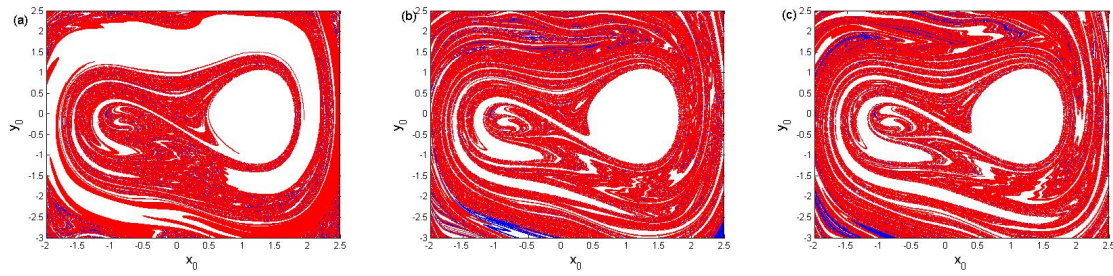


Figure 5: Effect of η on the basin of attraction: (a) $\eta = 0.3$, (b) $\eta = 2$ and (c) $\eta = 2.25$.

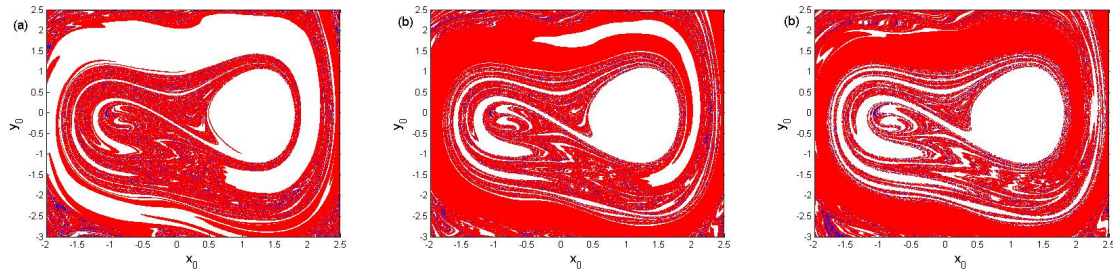


Figure 6: Effect of μ on the basin of attraction: (a) $\mu = 0.01$, (b) $\mu = 0.015$ and (c) $\mu = 0.02$

4. Bifurcation structures and routes to chaos

In this section, we investigate numerically via the fourth order Runge-Kutta integration algorithm, the eventual routes to chaos as well as the phenomenon of coexistence of attractors as certain parameters evolve. So, the bifurcation diagram and its corresponding lyapunov exponent versus the amplitude of the external excitation are plotted in Fig.7. The blue and red colors represent the bifurcation diagrams by scanning the parameter F upwards and downwards respectively. By comparing these two sets of data, we notice that system (5) displays monostability and bistability phenomena as well as the phenomenon of coexistence of attractors. Therefore the hysteresis phenomenon takes place in the system. These dynamical behaviors displayed by the bifurcation diagrams of Fig.7 are illustrated in Fig.8.

The effect of μ on the bifurcation diagram is examined in Fig.9. We notice that the domain where appears chaos increases where μ decreases. Moreover, the system vibrates from period-1 motion to chaos. This transition displays by the system represents a remarkable route to chaos. By comparing the two sets of data, we also notice that system (5) presents the phenomena of monostability, bistability and coexistence of attractors.

The influence of initial conditions as γ evolves is shown in Fig.10. We notice that system (5) can vibrate from period-3 motion to chaos. On the other hand, when we compare the three sets of data, we can conclude that system under consideration displays multiple coexisting attractors' behaviors. These complex dynamical behaviors are illustrated in Fig.11.

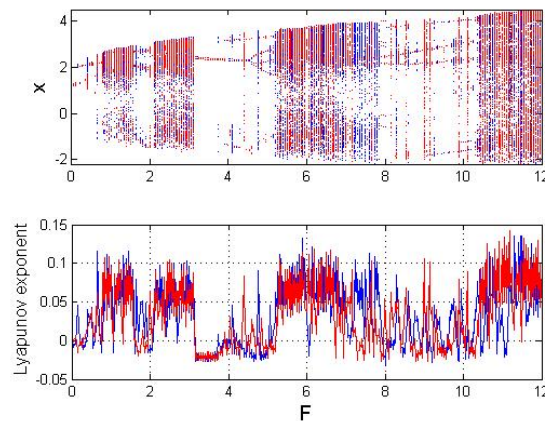


Figure 7: Bifurcation diagrams and its corresponding Lyapunov exponents versus F with the parameters $\alpha = -1, \beta = 0.85, \gamma = 0.3, \nu = 0.1, \omega = 1, \eta = 0.2$ and $\mu = 0.01$. Blue and red colors represent the bifurcation diagram by scanning F forward and downward respectively. The specific initial conditions are $(0.1, 0.1)$ (blue) and $(-0.1, -0.1)$ (red).

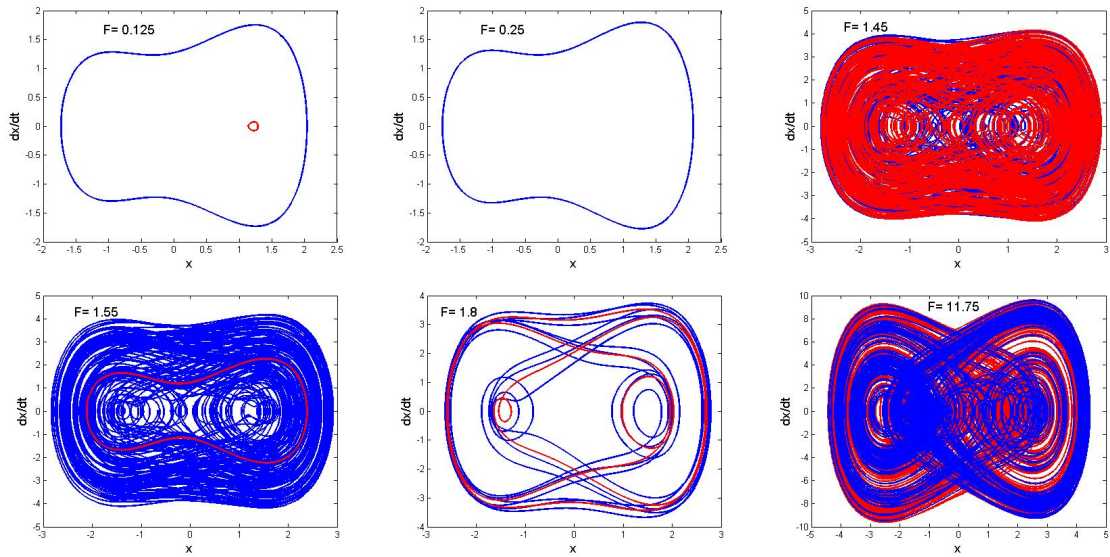


Figure 8: Phase portraits illustrating monstability, bistability and coexistence of attractors phenomena for several different values of F with the parameters of Fig.7.

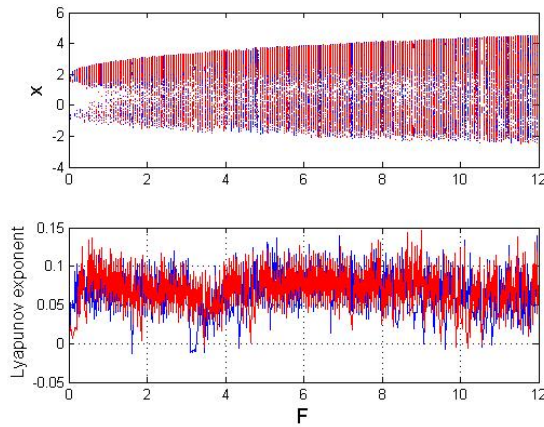


Figure 9: Bifurcation diagrams and its corresponding Lyapunov exponents versus F with the parameters of Fig.7 for $\mu = 0.001$.

5. Active control

5.1. Effects of the control on the horseshoe chaos

As it was shown above, the nonlinear chemical oscillations under consideration in this work present the chaotic states when it is subjected to an external periodic excitation. Among the proposed control strategies in the literature to suppress or enhance chaos in dynamic systems, we use here an active control to suppress or reduce this undesirable phenomenon that appears in our system. For this, we analyze the effects of this control on the Melnikov criterion for the appearance of chaos. The dynamics of the model is now described by the following set of differential equations:

$$\ddot{x} - \mu \left(v - x^2 + \eta x \dot{x} - \frac{1}{3} \eta^2 x^2 \right) \dot{x} + \alpha x + \beta x^3 - \gamma = F \cos(\omega t) + d_1 \dot{z} \tag{25}$$

$$\dot{z} = d_2 \dot{x} (1 - z) \tag{26}$$

where z is the control force, d_1 and d_2 represent the control gain parameters. The Melnikov function is now given by:

$$M(t_0) = A \pm BF \sin(\omega t_0) + d_1 I_6, \tag{27}$$

where $I_6 = -d_2 \int_{-\infty}^{\infty} y_h^2(z_h - 1) d\tau$ with $z_h = 1 - \exp(-d_2 x_h)$. Now, taking into account Eqs.(16) and the expression of z_h , the integral I_6 becomes:
$$I_6 = -\frac{4d_2 q^2 \sigma^5}{\beta^2} e^{-pd_2} \int_0^1 \frac{\zeta^2}{[p\sqrt{1-\zeta^2} \pm q]^4} \exp\left(-\frac{\sigma^2 d_2 \sqrt{2(1-\zeta^2)}}{\beta(p\sqrt{1-\zeta^2} \pm q)}\right) d\zeta.$$

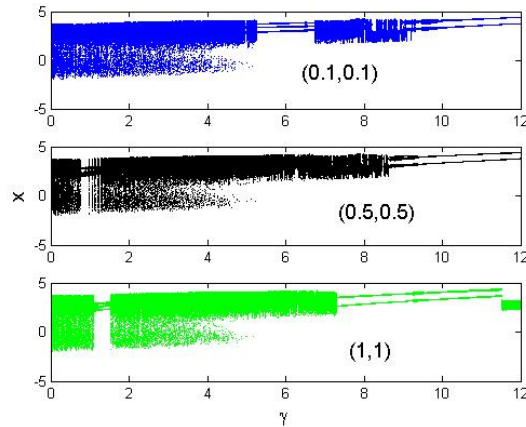


Figure 10: Effect of γ on the bifurcation diagram of the system (5) with the parameters of Fig.9 for $F = 5$.

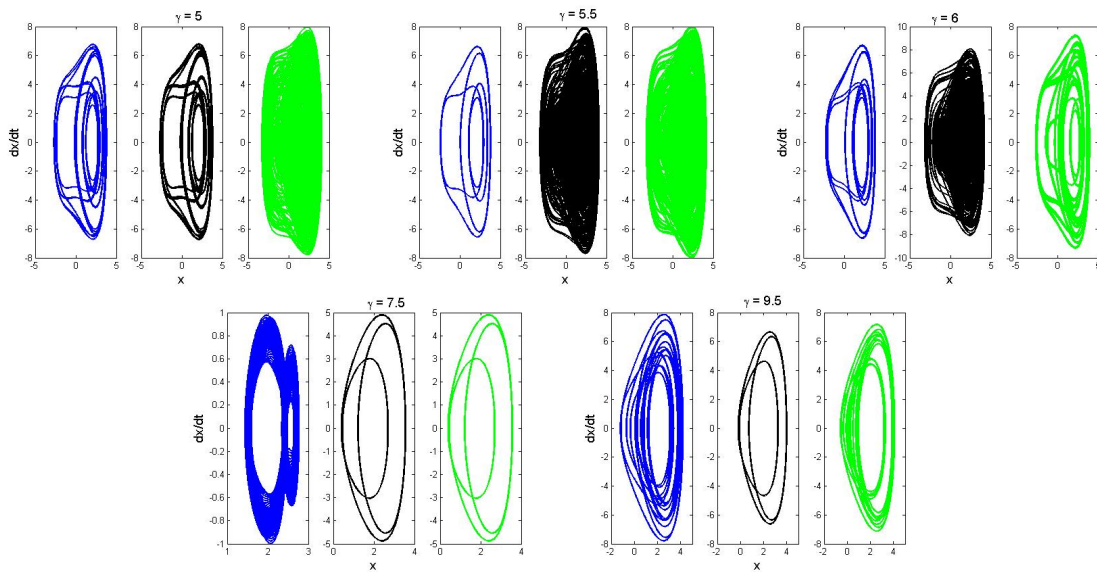


Figure 11: Phase portraits showing chaotic and periodic oscillations for several different values of γ with the parameters of Fig.10

Since it is difficult to evaluate the integral I_6 analytically, we obtained it numerically. If we set $M(t_0) = 0$ and recalling the previous calculations, the necessary condition for the appearance of the Melnikov chaos is given by:

$$F \geq F_{cr} = \left| \frac{A + d_1 I_6}{B} \right| \tag{28}$$

We have plotted in Fig.12 the regions in the space parameters where chaos is suppressed. These regions are II and IV. We have also investigated in Fig.13, the effects of the control parameters chosen in II and IV regions on the Melnikov threshold curve of the uncontrolled chemical system under consideration. From this figure, we clearly observe that the chaotic area decreases when the control is applied. In order to validate the analytical predictions, we have simulated numerically the set of Eqs. (25) and (26) to see the effects of the control parameters on the fractality of the basin of attraction. To this end, the obtained results are presented in Fig.14. We notice that when the control is applied with the value of the control gain parameters chosen in I and IV regions (for example $(d_1, d_2) = (0.85, 0.85)$ and $(d_1, d_2) = (-0.85, -0.85)$), the fractality disappears. However, in other regions, we clearly see that fractal structure exists. Therefore, we can confirm that the control is efficient in I and IV regions.

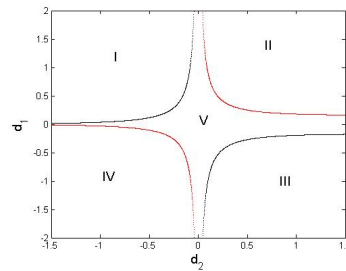


Figure 12: Domain in the space for the control of chaos with the parameters of Fig.3(c). Melnikov chaos disappears in II and IV.

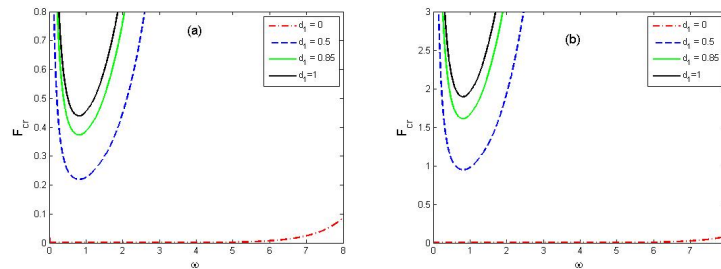


Figure 13: Effects of the control parameter d_1 on the Melnikov threshold curve of the uncontrolled chemical system with the parameters of Fig.2 for: (a) $d_2 = 0.85$ and (b) $d_2 = -0.85$

5.2. Suppression of chaotic oscillations

Our goal in this subsection is to investigate the control gain parameter values leading to a good suppression of chaos in nonautonomous chemical system given by Eq.(5). To this end, the effects of control gain parameters on bifurcation diagram of the system (5) are shown in Fig. 15. From this figure, we notice that as the control gain parameter d_1 increases and takes the value 3.0 with $d_2 = -0.85$, the chaotic oscillations disappear and the system displays periodic oscillations.

6. Conclusions

The analysis performed in this study aims to explore the dynamics and active control in nonlinear chemical oscillations modeled by a forced generalized Rayleigh oscillator with asymmetric potential. The originality of this work in the chaotic dynamics of nonlinear chemical system is brought by the presence of the impure and pure cubic damping terms of the type xx^2 and x^3 . The Melnikov criterion is applied to analytically determine Smale's horseshoes chaos. The basins of attraction are used to numerically verify the analytical results. The numerical simulations obtained are in good agreement with the analytical prediction given by the Melnikov technique. The regions in the control gain parameters space where the Melnikov chaos is suppressed are obtained. The bifurcation structures obtained via the fourth-order Runge Kutta integration algorithm show that the new nonautonomous chemical oscillator presents a rich variety of dynamical behaviors and remarkable transitions to chaos. The effects of control gain parameters on the behavior of a forced generalized Rayleigh oscillator governing the dynamic of nonlinear chemical oscillations are analyzed. It appears that for appropriate values of control gain parameters, the suppression of chaotic oscillations takes place.

References

- [1] I.R. Epstein, J.A. Pojman, An introduction to nonlinear chemical dynamics, *Oxford University Press*, (1998)
- [2] A. B. Çambel, An introduction to nonlinear chemical dynamics, *Academic Press*, (1993)
- [3] J. B. Buchler, H. Einhorn, Chaotic Phenomena in Astrophysics, *Annals of the New York Academy of Sciences*, Vol.497, No., (1987), pp.
- [4] S. Ghosh, D.S. Ray, Lincarard-type chemical oscillator, *Eur. Phys. J. B.*, Vol.87, No.65, (2014), pp.1-7
- [5] A.H. Nayfeh, D.T. Mook, Nonlinear Oscillations, *John Wiley and Sons*, (1979)
- [6] Garnett P. Williams, Chaos Theory Tamed, *Joseph HENRY Press*, (1997)
- [7] C. Hayashi, Nonlinear Oscillations in Physical Systems, *McGraw-Hill*, (1964)
- [8] F. Kaiser, Coherent Excitations in Biological Systems: Specific Effects in Externally Driven Self-Sustained Oscillating Biophysical Systems, *Springer-Verlag*, (1983).
- [9] B.R. Nana Nbenjo, R. Yamapi, Active control of extended Van der Pol equation, *Commun.Nonlinear Sci. Numer.Simul.*, Vol. 12,No., (2007), pp.1550—1559.
- [10] F. Ali, Stirring effects and phase-dependent inhomogeneity in chemical oscillations: The Belousov–Zhabotinsky reaction in a CSTR, *J. Phys. Chem.*, Vol. 101,No., (1997), pp.2304—2309.
- [11] M. Gruebelle and P. G. Wolynes, Vibrational energy flow and chemical reactions, *Accounts of Chemical Research*, Vol. 37, No., (2004), pp.261—267.
- [12] P. Sarkar, D. S. Ray, Vibrational antiresonance in nonlinear coupled systems, *Physical Review E*, Vol. 99, No., (2019), pp.1—7.
- [13] S. Strogatz, Nonlinear Dynamics and Chaos: With Applications to Physics, Biology, Chemistry, and Engineering, *Plingram Publisher Services*, (2014).
- [14] P.S. Landa, P.V.E. McClintock, VVibrational resonance, *Journal of Physics A: Mathematical General*, Vol. 33, No.45, (2000), pp.433—438.
- [15] M.S. Soliman, Basin boundaries with fractal and smooth accumulation properties in systems with single potential well, *Chaos, Solitons & Fractals*, Vol. 9, No.6, (1998), pp..
- [16] B.C. Bao, T. Jiang, Q. Xu, M. Chen, H.G. Wu, Y.H. Hu, Coexisting infinitely many attractors in active band-pass filter-based memristive circuit, *Nonlinear Dynamics*, Vol. 83, No.3, (2016), pp.1711–1723.
- [17] V. Patidar, A. Sharma, G. Purohit, Dynamical behavior of parametrically driven Duffing and externally driven Helmholtz-Duffing oscillators under nonlinear dissipation, *Nonlinear Dynamics*, Vol. 83, No.3,(2016), pp.75–88.

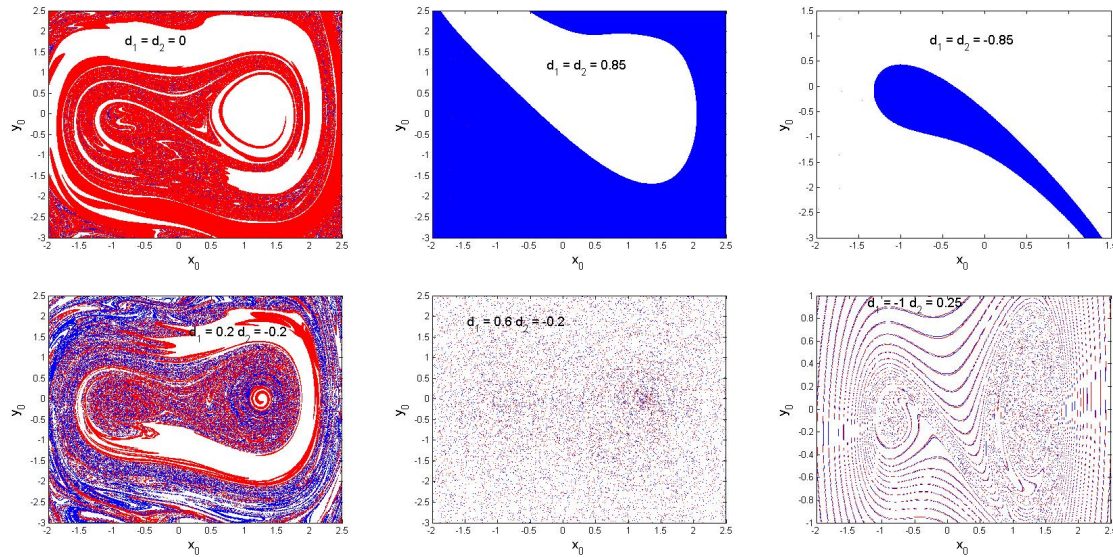


Figure 14: Basin of attraction showing the regions where the control is efficient (regions I and IV) and inefficient (regions I, III and V) with the parameter of Fig.5(c).

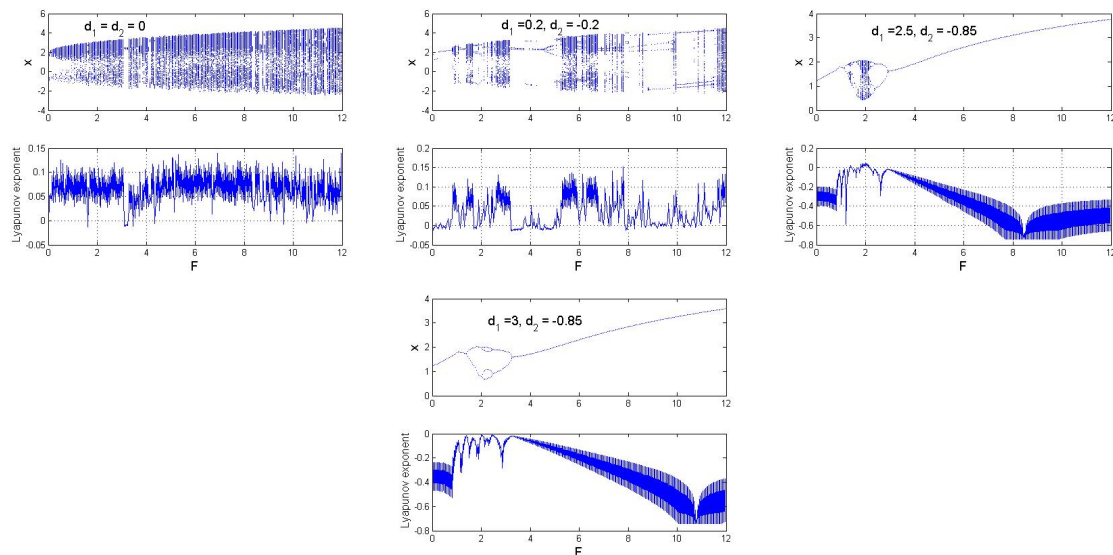


Figure 15: Effects of the control gain parameters on the amplitude of the nonautonomous system (5) with the parameters of Fig.9.

- [18] M.S. Siewe, H. Cao, M.A.F Sanjuan, Effect of nonlinear dissipation on the basin boundaries of a driven two-well Rayleigh-Duffing oscillator, *Chaos, Solitons & Fractal*, Vol. 39, No.10,(2009), pp.92–99.
- [19] B. Kaviya, R. Suresh, V.K. Chandrasekar, B. Balachandran, Influence of dissipation on extreme oscillations of a forced anharmonic oscillator, *International Journal of Non-Linear Mechanics*, Vol. , No.,(2020), pp.1–15.
- [20] C.A. Kitio Kwuimy, C. Nataraj, Melnikov's criteria, Parametric control of chaos, and stationary chaos occurrence in systems with asymmetric potential subjected to multiscale type excitation, *Chaos*, Vol.21 , No.,(2011), pp.1–12.
- [21] D.L. Olabodé, C.H. Miwadinou, A.V. Monwanou, J.B. Chabi Orou, Horseshoes chaos and its passive control in dissipative nonlinear chemical dynamics, *Phys. Scr.*, Vol.93 , No.,(2018), pp.1–12.
- [22] D.L. Olabodé, C.H. Miwadinou, V.A. Monwanou, J.B. Chabi Orou, Effects of passive hydrodynamics force on harmonic and chaotic oscillations in nonlinear chemical dynamics, *Physica D.*, Vol.386 , No.,(2019), pp.49–59.
- [23] D.L.Olabodé, B.Lamboni, J.B.Chabi Orou, Active control of chaotic oscillations in nonlinear chemical dynamics, *Journal of Applied Mathematics and Physics*, Vol.7 . No.,(2019), pp.547–558.
- [24] H.G. Enjiekadji, B.R. Nana Nbandjo, Melnikov's criteria, Passive aerodynamics control of plasma instabilities, *Commun Nonlinear Sci Numer Simulat*, Vol.17 , No.,(2012), pp.1779–1794.
- [25] A. Sambas, S.Vaidyanathan, Diandra C. Fransisca3, M.A. Mohamed, Trisnawan, D. Purwandari, A New Two-Wing Chaotic System with Line Equilibrium, its Analysis, Adaptive Synchronization and Circuit Simulation *International Journal of Engineering & Technology*, Vol.7 , No.4,(2018), pp.3739–3746.
- [26] A.V. Monwanou, A.A. Koukpémédji, C. Ainamon, P.R. Nwagoum Tuwa, C.H. Miwadinou, J.B. Chabi Orou, Nonlinear Dynamics in a Chemical Reaction under an Amplitude-Modulated Excitation: Hysteresis, Vibrational Resonance, Multistability, and Chaos *Complexity*, Article ID,(2020), pp.1–16.
- [27] R. Fangnon, C. Ainamon, A.V. Monwanou, C.H. Miwadinou, J.B. Chabi Orou, Nonlinear Dynamics of the Quadratic-Damping Helmholtz Oscillator *Complexity*, Article ID,(2020), pp.1–17.
- [28] J. Boissonade, P. De Keppel, Transitions from Bistability to Limit Cycle Oscillations Theoretical Analysis and Experimental Evidence in an Open Chemical System *Phys. Chem.*, Vol.84, No., (1980), pp.501–506.
- [29] I.R. Epstein, K. Showalter, Nonlinear Chemical Dynamics: Oscillations, Patterns, and Chaos, *J. Phys. Chem.*, Vol.100, No., (1996), pp.13132–13147.
- [30] B.P. Belousov, In *Oscillations and Travelling Waves in Chemical Systems*, Wiley, (1985).

- [31] C. H. Miwadinou, A.V. Monwanou, J. Yovogan, L. A. Hinvi, P. R. Nwagoum Tuwa, and J. B. Chabi Orou, Modeling nonlinear dissipative chemical dynamics by a forced modified Van der Pol-Duffing oscillator with asymmetric potential: chaotic behaviors predictions, *Chinese Journal of Physics*, Vol.56, No.3, (2018), pp.1089–1104.
- [32] Y.J.F. Kpomahou, L.A. Hinvi, J.A. Adéchinan, C.H. Miwadinou, Chaotic dynamics of a mixed Rayleigh–Lié nard oscillator driven by parametric periodic damping and external excitations, *Complexity*, Article ID, (2021), pp.1–18.
- [33] Y.J.F. Kpomahou, Adéchinan, Nonlinear dynamics and active control in a Liénard-type oscillator under parametric and external periodic excitations, *American Journal of Computational and Applied Mathematics*, Vol.10, No. 2, (2021), pp.48–61.
- [34] V.K.Melnikov, On the stability of the center for time periodic perturbations, *Transactions of the Moscow Mathematical Society*, Vol.12, No. 1, (1963), pp.1–57.
- [35] G. Cicogna, F.Papoff, Asymmetric doffing equation and the appearance of chaos, *Euro phys. Let*, Vol.3, No.9, (1987), pp.963–967.
- [36] I.S Gradshteyn, I.M. Ryzhik, Table of Integrals, Series, and Products, *Academic Press*, (2007).